ELSEVIER

Thermochimica Acta 375 (2001) 125–130

thermochimica acta

www.elsevier.com/locate/tca

Low-temperature heat capacity and thermochemical study of $[Re_2(Pro)_6(H_2O)_4](ClO_4)_6$ (Re = Nd, Gd; Pro = proline) crystals

Guang-Tao Li[a], Da-Shun Zhang[b], Lin Li[b], Zhi-Cheng Tan[a,*], Xin-Ming Wu[c], Shuang-He Meng[a]

[a]*Dalian Institute of Chemical Physics, Chinese Academy of Sciences, Dalian 116023, PR China*
[b]*Department of Chemistry, Changde Normal College, Changde 415000, PR China*
[c]*College of Chemistry and Environmental Science, Wuhan Univeristy, Wuhan 430072, PR China*

Received 17 July 2000; received in revised form 6 March 2001; accepted 6 April 2001

Abstract

The heat capacities of two solid complexes of rare-earth compounds with proline $[Re_2(Pro)_6(H_2O)_4](ClO_4)_6$ (Re = Nd, Gd; Pro = proline, $C_5H_9O_2N$), were measured with a high-precision automatic adiabatic calorimeter over the temperature range from 78 to 370 K. The heat capacity curves of the two complexes are smooth and similar in magnitude to each other except for a melting transition of $[Gd_2(Pro)_6(H_2O)_4](ClO_4)_6$ that occurred in the temperature range of 340–346 K with a peak temperature of 342.48 ± 0.01 K. The molar enthalpy and entropy of fusion of $[Gd_2(Pro)_6(H_2O)_4](ClO_4)_6$ were determined to be 26.104 ± 0.031 k J mol^{-1} and 76.23 ± 0.08 J K^{-1} mol^{-1}, respectively, on the basis of the heat capacity measurements. Thermal decompositions of the two complexes were studied through the thermogravimetry (TG) experiments and possible mechanisms of the decompositions were suggested according to the TG analysis. The molar combustion energies of the two complexes were determined to be 17010 ± 1.6 and 15630 ± 1.5 J mol^{-1} for $[Nd_2(Pro)_6(H_2O)_4](ClO_4)_6$ and $[Gd_2(Pro)_6(H_2O)_4](ClO_4)_6$, respectively, by means of oxygen-bomb calorimetric measurements.

Keywords: $[Re_2(Pro)_6(H_2O)_4](ClO_4)_6$ (Re = Nd, Gd, Pro = proline); Heat capacity; TG analysis; Combustion energy

1. Introduction

Solid complexes of rare-earth compounds with L-amino acids have been extensively studied in the last 20 years because of their biological effect [1]. Nearly 200 kinds of solid complexes have been prepared or studied in the last decade, and about 50 kinds of the complexes have their own crystallograms. However, until now, low-temperature heat capacities and thermodynamic properties of these complexes of rare-earth compounds with amino acids have not been reported in the literature.

Wang et al. [2] have prepared and characterized three single crystals of rare-earth perchlorates (Re = Pr, Er, Nd) with L-proline, and measured their crystal structures. In order to improve the processes of chemical synthesis of these substances and carry out relevant application and theoretical research, their thermodynamic properties are in urgent needs. In this paper, we report the low-temperature heat capacities of two complexes $[Nd_2(Pro)_6(H_2O)_4](ClO_4)_6$ and $[Gd_2(Pro)_6(H_2O)_4](ClO_4)_6$ over the temperature range

* Corresponding author. Fax: +86-411-4691570.
E-mail address: tzc@ms.dicp.ac.cn (Z.-C. Tan).

0040-6031/01/$ – see front matter
PII: S0040-6031(01)00525-1

from 75 to 370 K and the combustion energies at 298.15 K. In addition, a possible mechanism of thermal decomposition of the two complexes is proposed on the basis of thermogravimetry (TG) analysis.

2. Experimental

2.1. Sample preparation and characterization

Rare-earth oxides (Nd_2O_3, Gd_2O_3, 99.9%), perchloric acid (99%) and L-proline were used to prepare the experimental samples. First, the rare-earth oxides were dissolved in perchloric acid to obtain the aqueous solutions of the rare-earth perchlorates, then after mixing the aqueous solutions with L-proline at the mole ratio 1:3, the mixed solutions were stirred in the 80°C water bath for 6 h. When the mixed solutions were concentrated by evaporation, the solutions were cooled and filtered. The filtrates were placed into a desiccator with P_2O_5 until crystalline products were separated out from the solutions. The crystals were filtered out and washed with absolute alcohol for three times. Finally, the collected crystals were desiccated in a dryer until the mass of the crystals became constant.

The actual contents of the rare-earth ions obtained by EDTA titrimetric analysis were very close to the theoretic contents of rare-earth metal ions in the samples (the purities of the two samples are all higher than 99.70%). Thus, the crystals were pure enough to meet the requirements of the calorimetric measurements.

The melting points of $[Nd_2(Pro)_6(H_2O)_4](ClO_4)_6$ and $[Gd_2(Pro)_6(H_2O)_4](ClO_4)_6$ were determined to be 146.8–147.6 and 68.1–69.4°C, respectively, by means of a BY-1 microscopic melting point device manufactured by Yazawa Co. of Japan.

2.2. Adiabatic calorimetry

A high-precision automatic adiabatic calorimeter was used to measure the heat capacities of the samples. The principle and structure of the calorimeter have been described in detail elsewhere [3]. The calorimeter mainly consists of a sample cell, a platinum resistance thermometer, an electric heater, the inner and outer adiabatic shields, and two sets of eight-junction chromel–copel thermocouples and a vacuum can. The sample cell was a gold-plated container with an internal volume of about 6 cm^3, a Y-shaped gold-plated copper vane was placed in the sample cell to promote the heat conduction between the sample and the cell. The platinum resistance thermometer was tightly inserted in the copper sheath that was silver-soldered at the bottom of the sample cell, and the heater wire was evenly wound and fixed on the surface of the cell. After the sample was loaded in the sample cell and the lid with a copper capillary was sealed to the cell with an adhesive, the cell was filled with helium gas of 0.1 MPa to enhance the heat transfer within the cell during the heat capacity measurements. The temperature differences between the sample cell and the inner shield, and between the inner and outer shields were measured by two sets of chromel–copel thermocouples, respectively. The signals of the temperature differences were amplified and sent to a temperature controlling system to keep the two adiabatic shields at the same temperature as the sample cell. The vacuum can was evacuated to eliminate convection. The electrical energy introduced into the sample cell and the equilibrium temperature of the cell were periodically measured by use of an integration digital multi-meter (Model: 6030, Sabtronice, Switzerland), and the data were automatically collected and processed by an IBM-PC. The sample masses of $[Nd_2(Pro)_6(H_2O)_4](ClO_4)_6$ and $[Gd_2(Pro)_6(H_2O)_4](ClO_4)_6$ used for the measurements of heat capacities are 3.7435 and 2.9956 g, which are equivalent to 2.2715 and 1.7894 mmol, based on their corresponding molar mass 1648.04 and 1674.06 g mol^{-1}, respectively.

Prior to the heat capacity measurements of the complex samples, the reliability of the calorimetric apparatus was verified by heat capacity measurements of the reference standard material α-alumina. The sample mass used for the test was 2.8356 g. The deviations of our calibration results from the recommended values reported by Ditmars et al. of the National Bureau of Standards [4] are within ±0.1% in the temperature range of 80–400 K.

2.3. TG analysis

The TG measurements of the two samples were carried out by a thermogravimetric analyzer (Model:

DT-20B, Shimadzu, Japan) under static air. The mass of the sample used for TG analysis was 11.1 mg, and the heating rate was 10 K min^{-1}.

2.4. Measurement of combustion energy

The combustion energies of the two complex samples were measured with an oxygen-bomb calorimeter [5]. The method of combustion energy determination for the sample is the same as that for the combustion of benzoic acid. The calorimeter was calibrated with the reference standard material benzoic acid of molar percentage of 99.999. Benzoic acid has an isothermal combustion heat of 26476.0 ± 5.81 J g^{-1} at 298.15 K. The calibrated experimental results showed that there was an uncertainty of ±0.1% in the combustion calorimetric measurement system.

3. Results and discussion

3.1. Heat capacity

The experimental molar heat capacities of the two solid complexes are shown in Fig. 1 and listed in Tables 1 and 2, respectively. The molar heat capacities of the two samples are fitted to the following polynomials in reduced temperature (X), by means of the least square fitting.

For $[Nd_2(Pro)_6(H_2O)_4](ClO_4)_6$ solid complex over the temperature range of 80 to 370 K:

$$C_{p,m}\ (J\,K^{-1}\,mol^{-1}) = 1360.74589 + 654.34051X + 100.09839X^2 + 124.7034X^3 - 15.03159X^4$$

where, $X = (T - 223.7)/145.7$, and T is the absolute temperature.

The maximum deviation of experimental point from the fitted curve is within ±0.15%.

For $[Gd_2(Pro)_6(H_2O)_4](ClO_4)_6$ solid complex over the temperature range of 80 to 310 K:

$$C_{p,m}\ (J\,K^{-1}\,mol^{-1}) = 1244.44876 + 539.06522X + 79.2791X^2 + 49.14951X^3 - 90.49149X^4$$

where, $X = (T - 195.3)/113.8$, and T is the absolute temperature.

The maximum deviation of experimental points from the fitted curve is within ±0.12%.

From Fig. 1, it can be seen that the heat capacities of the sample $[Nd_2(Pro)_6(H_2O)_4](ClO_4)_6$ increase with increasing temperature in a smooth and continuous

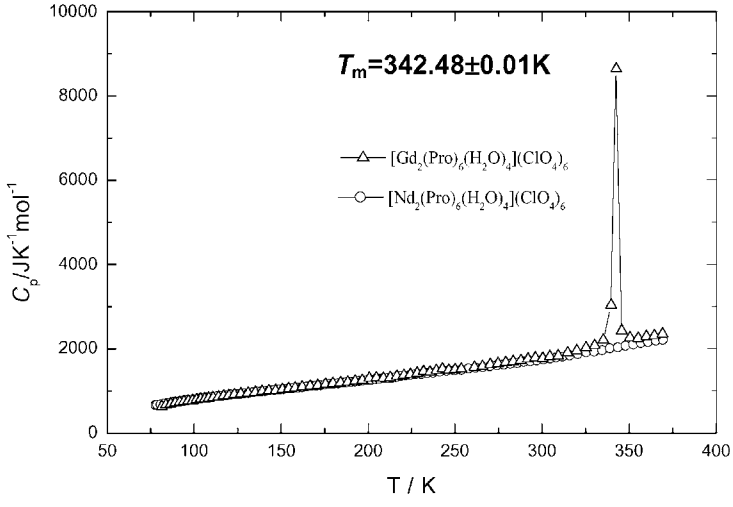

Fig. 1. Experimental heat capacity curves of $[Nd_2(Pro)_6(H_2O)_4](ClO_4)_6$ and $[Gd_2(Pro)_6(H_2O)_4](ClO_4)_6$ single crystals.

Table 1
The experimental molar heat capacities of $[Nd_2(Pro)_6(H_2O)_4](ClO_4)_6$[a]

T (K)	C_p (J K^{-1} mol^{-1})	T (K)	C_p (J K^{-1} mol^{-1})	T (K)	C_p (J K^{-1} mol^{-1})	T (K)	C_p (J K^{-1} mol^{-1})
77.971	658.24	136.237	974.61	197.188	1243.37	273.923	1604.50
78.914	665.90	138.640	984.28	199.554	1250.70	277.855	1621.21
80.908	675.11	141.018	992.77	201.903	1263.99	281.749	1640.90
83.087	694.08	143.370	1006.64	204.236	1273.74	285.610	1656.73
85.504	712.33	145.941	1017.30	206.557	1285.42	289.433	1688.24
87.864	723.42	148.729	1028.51	208.865	1296.24	293.193	1702.75
90.168	739.48	151.488	1040.56	211.163	1300.55	296.956	1718.33
92.422	754.93	154.221	1055.28	213.449	1310.39	300.680	1741.30
94.630	770.79	156.927	1063.42	215.980	1325.47	304.368	1763.82
96.800	779.45	159.609	1073.42	218.752	1343.15	308.018	1786.45
99.350	793.99	162.265	1086.78	221.501	1358.58	311.633	1809.08
102.270	810.21	164.895	1099.60	224.228	1373.66	315.816	1841.49
105.124	830.55	167.501	1111.77	227.250	1389.57	320.565	1871.34
107.926	844.46	170.085	1124.53	230.643	1401.19	325.250	1907.79
110.680	855.63	172.666	1133.33	233.962	1420.95	329.876	1932.57
113.393	868.61	175.173	1144.84	237.355	1431.99	334.459	1961.79
116.063	881.74	177.693	1158.13	241.117	1448.26	338.993	2012.37
118.696	895.28	180.193	1167.21	245.321	1463.36	343.486	2037.31
121.293	908.45	182.676	1180.67	249.526	1481.96	347.924	2070.55
123.856	917.79	185.138	1192.63	253.656	1501.13	352.365	2103.35
126.387	928.03	187.581	1200.37	257.809	1529.98	356.714	2132.76
128.886	940.53	190.007	1209.98	261.894	1543.58	361.008	2159.40
131.358	950.32	192.415	1224.89	265.943	1559.56	365.253	2184.71
133.809	964.19	194.808	1231.64	269.954	1580.25	369.463	2211.16

[a] Molar mass: $M = 1648.04$ g mol^{-1}.

manner. No phase transition or thermal anomaly was observed in the whole temperature range, indicating that this complex is stable in the above range. The heat capacity curve of $[Gd_2(Pro)_6(H_2O)_4](ClO_4)_6$ is similar to that of $[Nd_2(Pro)_6(H_2O)_4](ClO_4)_6$ in the temperature range from 78 to 340 K. However, a melting peak at about 342 K was observed for the $[Gd_2(Pro)_6(H_2O)_4](ClO_4)_6$ sample.

3.2. The melting point, molar enthalpy and entropy of fusion of $[Gd_2(Pro)_6(H_2O)_4](ClO_4)_6$

For the $[Gd_2(Pro)_6(H_2O)_4](ClO_4)_6$ sample, the melting point was determined from the heat capacity measurements by a progressive approach with step-by-step heating. The peak temperature of the heat capacity curve (Fig. 1) of the sample, 342.48± 0.01 K, was selected to be the melting point T_m.

The molar enthalpy ΔH_m and entropy ΔS_m of fusion of the $[Gd_2(Pro)_6(H_2O)_4](ClO_4)_6$ sample can be derived from the heat capacity data, according to the following Eqs. (1) and (2):

$$\Delta H_m = \frac{[Q - n\int_{T_i}^{T_m} C_p(S)dT - n\int_{T_m}^{T_f} C_p(L)dT - \int_{T_i}^{T_f} H_0 dT]}{n} \quad (1)$$

$$\Delta S_m = \frac{\Delta H_m}{T_m} \quad (2)$$

Where, T_i is a temperature slightly lower than the initial melting temperature, T_f a temperature slightly higher than the final melting temperature, Q the total energy introduced to the sample and container from T_i to T_f, H_0 the heat capacity of the sample cell from T_i to T_f, $C_p(S)$ the heat capacity of the sample in solid phase from T_i to T_m, $C_p(L)$ the heat capacity of the sample in liquid phase from T_m to T_f, and n is molar amount of the sample.

We obtained the values: $\Delta H_m = 26.104 \pm 0.031$ kJ mol^{-1}; $\Delta S_m = 76.23 \pm 0.08$ J K^{-1} mol^{-1}.

Table 2
The experimental molar heat capacities of $[Gd_2(Pro)_6(H_2O)_4](ClO_4)_6$[a]

T (K)	C_p (J K^{-1} mol^{-1})	T (K)	C_p (J K^{-1} mol^{-1})	T (K)	C_p (J K^{-1} mol^{-1})	T (K)	C_p (J K^{-1} mol^{-1})
81.566	625.33	143.019	1001.95	228.108	1419.02	310.111	1785.20
83.943	663.34	146.876	1010.02	231.841	1458.63	314.141	1810.44
86.642	686.71	150.676	1033.73	235.546	1447.05	318.120	1860.28
89.266	709.71	154.416	1053.36	239.222	1483.49	322.044	1900.00
91.827	725.62	158.102	1070.54	242.845	1519.12	325.918	1957.99
94.333	742.06	162.201	1095.72	246.448	1493.48	329.729	2033.31
96.7906	754.78	166.709	1110.65	250.047	1505.14	336.329	2190.45
99.207	766.31	171.157	1134.79	253.613	1523.58	338.448	2406.09
101.579	786.16	175.547	1153.69	257.954	1544.11	340.303	3273.67
103.905	800.51	179.872	1177.77	261.200	1563.57	341.634	6265.56
106.193	813.82	184.136	1193.57	265.718	1583.16	342.481	9148.26
108.449	828.74	188.354	1209.03	270.195	1624.17	343.656	3479.67
111.094	844.90	192.527	1230.45	274.623	1652.33	345.598	2128.80
114.117	858.09	196.650	1248.66	279.009	1674.76	347.828	2143.99
117.084	878.52	200.730	1303.84	283.346	1692.75	350.051	2151.32
120.002	891.26	204.781	1305.83	287.632	1720.29	352.959	2193.16
123.170	908.41	208.786	1302.67	289.280	1671.22	356.534	2220.91
126.967	930.56	212.738	1318.22	293.548	1699.31	360.070	2240.88
131.085	949.29	216.647	1344.99	297.761	1706.51	364.174	2272.50
135.130	967.88	220.510	1367.55	301.923	1746.29	368.839	2290.01
139.107	988.44	224.330	1392.21	306.038	1763.53	369.098	2294.27

[a] Molar mass: $M = 1674.06$ g mol^{-1}.

3.3. The results of TG/DTG analysis of the samples

The TG/DTG curves of the two samples are shown in Figs. 2 and 3, respectively. It can be seen from TG/DTG curves that three steps exist in the process of the thermal decompositions for each sample. Possible mechanisms of the thermal decomposition may be deduced as following, according to the mass loss in each step:

$$[Nd_2(Pro)_6(H_2O)_4](ClO_4)_6 \times \underset{2.19\%\,(2.54\%)}{\overset{80-110^{\circ}C}{\longrightarrow}} [Nd_2(Pro)_6(H_2O)_2](ClO_4)_6 \times \underset{43.01\%\,(42.73\%)}{\overset{230-348^{\circ}C}{\longrightarrow}} [Nd_2(H_2O)](ClO_4)_6 \times \underset{24.39\%\,(24.00\%)}{\overset{348-580^{\circ}C}{\longrightarrow}} 2NdCl_3$$

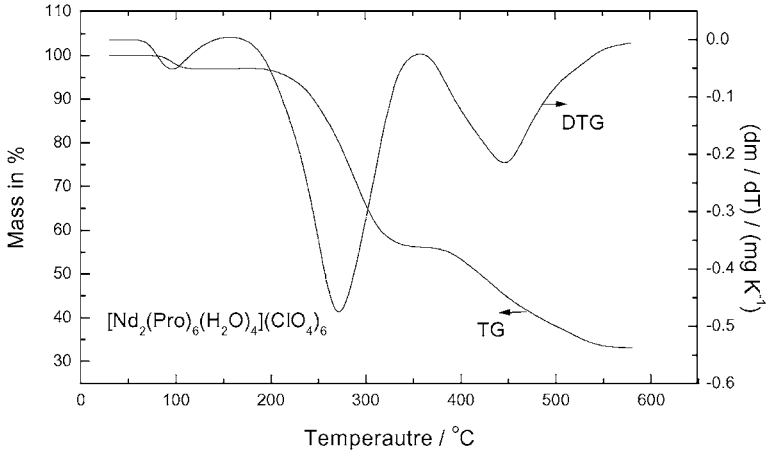

Fig. 2. TG/DTG curves of $[Nd_2(Pro)_6(H_2O)_4](ClO_4)_6$ sample.

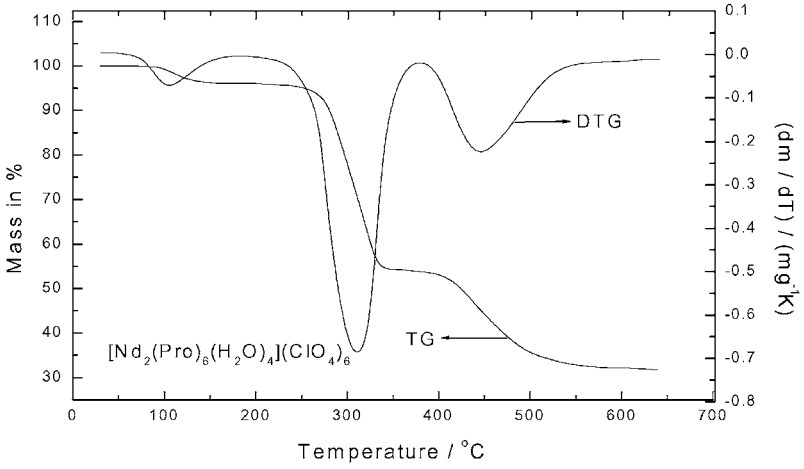

Fig. 3. TG/DTG curves of $[Gd_2(Pro)_6(H_2O)_4](ClO_4)_6$ sample.

$$[Gd_2(Pro)_6(H_2O)_4](ClO_4)_6 \times \underset{3.23\%\,(3.09\%)}{\overset{80-120^{\circ}C}{\longrightarrow}} [Gd_2(Pro)_6(H_2O)](ClO_4)_6 \times \underset{48.08\%\,(48.18\%)}{\overset{250-375^{\circ}C}{\longrightarrow}} 2(GdClO_3)_3 \times \underset{20.48\%\,(21.45\%)}{\overset{375-640^{\circ}C}{\longrightarrow}} GdOCl \cdot GdCl_3$$

The mass-loss percentages in the brackets are the calculated theoretical values.

3.4. Combustion energies of the samples

The molar combustion energies of the two complexes were determined to be 17010 ± 1.6 J mol^{-1} for $[Nd_2(Pro)_6(H_2O)_4](ClO_4)_6$ and 15630 ± 1.5 J mol^{-1} for $[Gd_2(Pro)_6(H_2O)_4](ClO_4)_6$ at 298.15 K, respectively, by oxygen-bomb combustion calorimetry. The value of combustion energy of the former is slightly higher than that of the latter, which may account for the fact that the interaction between Gd^{3+} and the two kinds of ligands (proline and H_2O) is a little stronger than that between Nd^{3+} and the same ligands (proline and H_2O) because of "lanthanide contraction" effect that makes the ion radius of Gd^{3+} (0.119 nm [6]) slightly smaller than that of Nd^{3+}(0.125 nm [6]).

References

[1] B.S. Guo, Rare Earth 20 (1999) 64.
[2] Z.L. Wang, C.J. Niu, N.H. Hu, J.Z. Ni, Acta Chim. Sinica 51 (1993) 257.
[3] Z.C. Tan, L.X. Zhou, S.X. Chen, Sci. Sin. B 26 (1983) 1014.
[4] D.A. Ditmars, S. Ishihara, S.S. Chang, G. Bernstein, E.D. West, J. Res. Nat. Bur. Stand. 87 (1982) 159.
[5] L.M. Zhang, Z.C. Tan, S.D. Wang, D.Y. Wu, Thermochim. Acta 299 (1997) 13.
[6] R.D. Shannon, Acta Crystallogr. A 32 (1976) 751.